

We are IntechOpen, the world's leading publisher of Open Access books Built by scientists, for scientists

6,900

Open access books available

185,000

International authors and editors

200M

Downloads

Our authors are among the

154

Countries delivered to

TOP 1%

most cited scientists

12.2%

Contributors from top 500 universities



WEB OF SCIENCE™

Selection of our books indexed in the Book Citation Index
in Web of Science™ Core Collection (BKCI)

Interested in publishing with us?
Contact book.department@intechopen.com

Numbers displayed above are based on latest data collected.
For more information visit www.intechopen.com



Simulation of Hydrodynamics and Mass Transfer in a Valve Tray Distillation Column Using Computational Fluid Dynamics Approach

A. Jafari¹, S.M. Mousavi^{2*} H. Motesaffi²,
H. Roohian² and H. Hamed Sangari³

¹Department of Planning and Development,
National Petrochemical Company, Tehran,

²Biotechnology Group, Chemical Engineering Department,
Tarbiat Modares University, Tehran,

³R & T Management Department,
National Iranian Oil Refining and Distribution Company, Tehran,
Iran

1. Introduction

Distillation is a widely used method to separate liquid mixtures into their components and has been applied in many separation processes such as those in petroleum, petrochemical, chemical and related industries. It shares a large portion of the capital investment, and is the largest consumer of energy in those industries. It is also commonly recognized that distillation is a very important process in today's industry and will continue to be in the future (You, 2004). Tray column is widely used as distillation column in chemical and petrochemical industry. It has some advantages compared with packed column, such as easy maintainability, low cost, convenient feed and side-stream withdrawal, and reliability for high pressure and high viscosity liquid. Numerous studies were carried out on tray columns and many different types of tray have been developed. Among them, valve tray is one of the most effective ones, and it plays an important role in commercial production due to its flexibility in handling a wide range of vapour throughputs. As the gas horizontally blows out of the valves and has a long hold-up time, the valve has low entrainment and higher average operating efficiency than sieve trays which had been in use before (Lianghua et al., 2008; Li *et al.*, 2009).

Even if valve tray columns are widely used in distillation processes separating liquid mixtures, a bottleneck that impedes the further improvement of these column internals is the fact that little is known about the detailed flow field through the valves on the tray for a given geometry under different operation conditions. The main reason is the complex flow

* Corresponding author at: Biotechnology Group, Chemical Engineering Department, Tarbiat Modares University, Jālal Al Ahmad highway, Tehran, Iran. Tel.: +98 21 82884917. Fax: 82884931, E-mail address: mousavi_m@modares.ac.ir (S.M. Mousavi).

behaviours on the tray deck. For example, although it is well known that the liquid flow pattern, or velocity distribution, is a very important factor in distillation tray design, the details of the extremely complex hydrodynamic processes on trays still do not seem to be completely understood (Hirschberg *et al.*, 2005; Lianghua *et al.*, 2008). In contrast with the importance and common use of valve tray columns, due to the complex geometry of their valves, there is lack of report about simulating the hydrodynamics of valve trays by using computational fluid dynamics (Li *et al.*, 2009).

In the recent years, computational fluid dynamics (CFD) has attracted the attention of researchers as a powerful tool for fluid-flow phenomena in various devices. It is possible to use CFD method to simulate the complex fluid flow performance on trays. Compared to experimental method, CFD has the flexibility of testing different flow geometry and system conditions without suffering appreciable cost. At present, numerical simulation is mainly focused on the liquid flow field (Li *et al.*, 2009; Zhang & Yu, 1994; Liu *et al.*, 2000) or the gas-liquid two-phase flow (Delnoij *et al.*, 1999; Deen *et al.*, 2001; Buwa & Ranade 2002; Van Baten & Krishna, 2000) on a tray.

Since the liquid distribution on a valve tray is complex in its structure influenced by the hydrodynamics behaviour of gas through the bubble element, it is very important to study the hydrodynamics behaviour of the gas using CFD (Lianghua *et al.*, 2008). The tray design based on computational fluid dynamics foundation is obviously superior to that based on experience or rough estimation, especially for the case of scaling up a column to large diameter (You, 2004). The idea of using CFD to incorporating the prediction of tray efficiency relies on the fact that the hydrodynamics is an essential influential factor for mass transfer in both interfacial and bulk diffusions, which could be understood by the effect of velocity distribution on concentration profile. This, in fact, opens an issue on the computation for mass transfer prediction based on the fluid dynamics computation (Sun *et al.*, 2007). Several recent publications have established the potential of CFD for describing tray hydraulics and tray performance (Wijn, 1996; Mehta *et al.*, 1998; Fischer & Quarini, 1998; Yu *et al.*, 1999; Krishna & van Baten, 1999; Liu *et al.*, 2000; Ling *et al.*, 2004; Rahbar *et al.*, 2006; Li *et al.*, 2009; Alizadehdakhel, 2010).

The experts cited transport phenomena such as fluid flow, heat and mass transfer, and multi-phase flow as subjects that are insufficiently understood. In recent years there has been considerable academic and industrial interest in the use of computational fluid dynamics (CFD) to model two-phase flows in process equipment. The use of CFD models for gas-liquid bubble columns has also evoked considerable interest in recent years and both Euler-Euler and Euler-Lagrange frameworks have been employed for the description of the gas and liquid phases (Van Baten & Krishna, 2000). Mehta *et al.* (1998) have analysed the liquid phase flow patterns on a sieve tray by solving the time-averaged equations of continuity of mass and momentum only for the liquid phase. Interactions with the vapour phase are taken account by use of interphase momentum transfer coefficients determined from empirical correlations. Yu *et al.* (1999) attempted to model the two-phase flow behaviour using a two-dimensional model, focussing on the description of the hydrodynamics along the liquid flow path, ignoring the variations in the direction of gas flow along the height of the dispersion. Fischer and Quarini (1998) have attempted to describe the three-dimensional transient gas-liquid hydrodynamics. An important key assumption made in the simulations of Fischer and Quarini concerns the drag coefficient;

these authors assumed a constant drag coefficient of 0.44, which is appropriate for uniform bubbly flow.

As a result of the development of computer technology beginning in the sixties of last century, the computational fluid dynamics and heat transfer were initiated on the basis of closure of the differential equations of momentum and heat transfer respectively by the fluid dynamic researchers and mechanical engineers. Nevertheless, in the chemical engineering work, the prediction of concentration field is equally important, and the task of such development, which may be regarded as computational mass transfer, is naturally relied on the investigation by the chemical engineers. Recently, works on computational mass transfer have been reported covering its basic ground and various applications. The early research on the numerical simulation of concentration distribution was reported in 1960s, almost at the same time when CFD was developed (McFarlane et al., 1967; Farouqali & Stahl, 1969), but the simulation of concentration and temperature distributions depended largely on the pattern of velocity distribution by CFD. Yu et al. studied the concentration field on a sieve tray by applying the CFD method to solve the flow and mass transfer equations with the assumption of constant equilibrium ratio of the separated substance in the mixture. They obtained the mass transfer efficiency in terms of effectiveness of the tray. But their assumption of constant equilibrium ratio would lead to a large deviation in the case of having wide range of tray concentration. Therefore, a variable equilibrium ratio is adopted to recalculate the concentration field on the tray in this study (Yu et al., 1999). You analysed quantitatively the dependence of mass transfer performance of sieve distillation tray on the physical properties of fluid and tray flow patterns and discussed the ways to improve the efficiency of distillation sieve tray (You, 2004). Wang et al. presented a three-dimensional CFD model for describing the liquid-phase flow and concentration distribution on a distillation column tray. They considered both volume fractions of gas and liquid as well as the interfacial forces and the interphase mass transfer item. Simulations of three-dimensional liquid flow and the concentration distribution were carried out on both a single tray and all trays of a distillation column with 10 sieve trays under total reflux and the prediction by the present model for liquid flow on a single tray was confirmed by the experimental measurements (Wang et al., 2004). Sun et al. demonstrated the feasibility of the simplified computational mass transfer model for distillation column simulation, and compared the simulation results with the experimental data taken from literatures. They showed that by applying the modified model to the simulation of a commercial scale distillation tray column, predicted concentration at the outlet of each tray and the tray efficiency were satisfactorily confirmed by the published experimental data (Sun et al., 2007). The computational mass transfer under investigation now aims to the prediction of concentration distribution of complex fluid systems with simultaneous mass, heat and momentum transports and/ or chemical reactions in chemical processes (Xigang & Guocong, 2008).

The purpose of this research was to develop a three-dimensional CFD modeling, within the two-phase Eulerian framework, to understand the hydrodynamics and mass transfer of valve trays in a distillation column. Velocity distributions, clear liquid height, phases volume fractions, and separation of materials under unsteady state conditions were predicted. The main objective of this work was to consider gas-liquid mass transfer (species distribution for each phase) for cyclohexane-n-heptane separation in a single valve tray distillation column.

2. Mathematical formulation

2.1 Governing equations

In this research Eulerian method was used to predict the behaviour of gas-liquid in a valve tray. The governing equations were solved sequentially. The non-linear governing equations were linearized to produce a system of equations for the dependent variables in every computational cell. The resulting linear system was then solved to yield an updated flow-field solution. A point implicit (Gauss-Seidel) linear equation solver was used in conjunction with an algebraic multigrid method to solve the resulting scalar system of equations for the dependent variable in each cell.

The continuity equation for phase q is:

$$\frac{\partial}{\partial t}(\alpha_q \rho_q) + \nabla \cdot (\alpha_q \rho_q \vec{v}_q) = 0 \quad (1)$$

Where α , ρ and \vec{v} shows volume fraction, density and velocity, respectively. The description of the multiphase flow as an interpenetrating continuum incorporated the concept of volume fraction, denoted by α_q . The volume fractions represent the space occupied by each phase, and the laws of conservation of mass and momentum are satisfied by each phase individually. The derivation of the conservation equations can be done by calculating the ensemble average of the local instantaneous balance for each of the phases or by using the mixture theory approach. It is assumed that density is constant, then the continuity equation (Eq. (1)) can be written as Eq. (2), and the volume fraction of each phase can be calculated via this equation:

$$\frac{\partial}{\partial t}(\alpha_q) + \nabla \cdot (\alpha_q \vec{v}_q) = 0 \quad (2)$$

The momentum balance for phase q yields:

$$\frac{\partial}{\partial t}(\alpha_q \rho_q \vec{v}_q) + \nabla \cdot (\alpha_q \rho_q \vec{v}_q \vec{v}_q) = -\alpha_q \nabla P + \nabla \cdot \bar{\bar{\tau}}_q + \alpha_q \rho_q \vec{g} + \sum_{p=1}^n (\bar{\bar{R}}_{pq}) + \alpha_q \rho_q (\bar{\bar{F}}_q) \quad (3)$$

where t , P , \vec{g} , $\bar{\bar{\tau}}$, $\bar{\bar{R}}_{pq}$, and $\bar{\bar{F}}_q$ represents time, pressure, gravity, stress-strain tensor, interphase force, and body force, respectively. Here n is number of phases. The q phase stress-strain tensor ($\bar{\bar{\tau}}_q$) was defined as follow:

$$\bar{\bar{\tau}}_q = \alpha_q \mu_q (\nabla \vec{v}_q + \nabla \vec{v}_q^T) + \alpha_q (\lambda_q - \frac{2}{3} \mu_q) \nabla \cdot \vec{v}_q \bar{\bar{I}} \quad (4)$$

where μ and λ_q are dynamic viscosity and bulk viscosity of phase q , respectively. The interphase force, $\bar{\bar{R}}_{pq}$, depended on the friction, pressure, cohesion, and other effects and was subjected to the conditions that $\bar{\bar{R}}_{pq} = -\bar{\bar{R}}_{qp}$, $\bar{\bar{R}}_{qq} = 0$ and that

$$\sum_{p=1}^n \bar{\bar{R}}_{pq} = \sum_{p=1}^n K_{pq} (\vec{v}_p - \vec{v}_q) \quad (5)$$

where K_{pq} (K_{qp}) is the interphase momentum exchange coefficient; and it tends to zero whenever the primary phase is not present within the domain.

In simulations of the multiphase flow, the lift force can be considered for the secondary phase (gas). This force is important if the bubble diameter is very large. It was assumed that the bubble diameters were smaller than the distance between them, so the lift force was insignificant compared with the other forces, such as drag force. Therefore, there was no reason to include this extra term.

The exchange coefficient for these types of gas-liquid mixtures can be written in the following general form:

$$K_{pq} = \frac{\alpha_q \alpha_p \rho_p f}{\tau_p} \quad (6)$$

where f and τ_p are the drag function and relaxation time, respectively. f can be defined differently for the each of the exchange-coefficient models. Nearly all definitions of f include a drag coefficient that is based on the relative Reynolds number. In this study the basic drag correlation implemented in FLUENT (**Schiller-Naumann**) was used in order to predict the drag coefficient.

In comparison with single-phase flows, the number of terms to be modeled in the momentum equations in multiphase flows is large, which complicates the modeling of turbulence in multiphase simulations.

In the present study, standard $k-\varepsilon$ turbulence model was used. The simplest "complete models" of turbulence are two-equation models in which the solution of two separate transport equations allows the turbulent velocity and length scales to be independently determined. Economy, and reasonable accuracy for a wide range of turbulent flows explain popularity of the standard $k-\varepsilon$ model in industrial flow and heat transfer simulations. It is a semi-empirical model, and the derivation of the model equations relies on phenomenological considerations and empiricism (FLUENT 6.2 Users Guide, 2005).

The equations k and ε that describe the model are as follows:

$$\frac{\partial}{\partial t}(\rho_m k) + \nabla \cdot (\rho_m \vec{v}_m k) = \nabla \cdot \left(\frac{\mu_{t,m}}{\sigma_k} \nabla k \right) + G_{k,m} - \rho_m \varepsilon \quad (7)$$

and

$$\frac{\partial}{\partial t}(\rho_m \varepsilon) + \nabla \cdot (\rho_m \vec{v}_m \varepsilon) = \nabla \cdot \left(\frac{\mu_{t,m}}{\sigma_\varepsilon} \nabla \varepsilon \right) + \frac{\varepsilon}{k} (C_{1\varepsilon} G_{k,m} - C_{2\varepsilon} \rho_m \varepsilon) \quad (8)$$

where k and ε shows turbulent kinetic energy and dissipation rate, respectively; and $C_{1\varepsilon}$, $C_{2\varepsilon}$, σ_k and σ_ε are parameters of the model. The mixture density and velocity, ρ_m and \vec{v}_m , are computed from:

$$\rho_m = \sum_{i=1}^N \alpha_i \rho_i \quad (9)$$

and

$$\bar{v}_m = \frac{\sum_{i=1}^N \alpha_i \rho_i \bar{v}_i}{\sum_{i=1}^N \alpha_i \rho_i} \quad (10)$$

The turbulent viscosity $\mu_{t,m}$ is computed from:

$$\mu_{t,m} = \rho_m C_\mu \frac{k^2}{\varepsilon} \quad (11)$$

The production of turbulent kinetic energy $G_{k,m}$ is computed from:

$$G_{k,m} = \mu_{t,m} (\nabla \bar{v}_m + (\nabla \bar{v}_m)^T) : \nabla \bar{v}_m \quad (12)$$

2.2 Species transport equations

To solve conservation equations for chemical species, software predicts the local mass fraction of each species, Y_i , through the solution of a convection-diffusion equation for the i^{th} species. This conservation equation takes the following general form:

$$\frac{\partial}{\partial t}(\rho Y_i) + \nabla \cdot (\rho v Y_i) = -\nabla \cdot \mathbf{j} + R_i + S_i \quad (13)$$

where R_i is the net rate of production of species i by chemical reaction and here it is zero. S_i is the rate of creation by addition from the dispersed phase plus any user-defined sources. An equation of this form will be solved for $N - 1$ species where N is the total number of fluid phase chemical species present in the system. Since the mass fraction of the species must sum to unity, the N^{th} mass fraction is determined as one minus the sum of the $N - 1$ solved mass fractions.

In Equation (13), \mathbf{j} is the diffusion flux of species i , which arises due to concentration gradients. By default, FLUENT uses the dilute approximation, under which the diffusion flux can be written as:

$$\mathbf{j} = -\rho D_{i,m} \nabla Y_i \quad (14)$$

Here $D_{i,m}$ is the diffusion coefficient for species i in the mixture.

3. Numerical implementation

3.1 Simulation characteristics

In the present work, commercial grid-generation tools, GAMBIT 2.2 (FLUENT Inc., USA) and CATIA were used to create the geometry and generate the grids. The use of an adequate number of computational cells while numerically solving the governing equations over the solution domain is very important. To divide the geometry into discrete control volumes, more than 5.7×10^5 3-D tetrahedral computational cells and 37432 nodes were used. Schematic of the valve tray is shown in figure 1.

The commercial code, FLUENT, have been selected for simulations, and Eulerian method implemented in this software; were applied. Liquid and gas phase was considered as

continuous and dispersed phase, respectively. The inlet flow boundary conditions of gas and liquid phase was set to inlet velocity. The liquid and gas outlet boundaries were specified as pressure outlet fixed to the local atmospheric pressure. All walls assumed as no slip wall boundary. The gas volume fraction at the inlet holes was set to be unity.

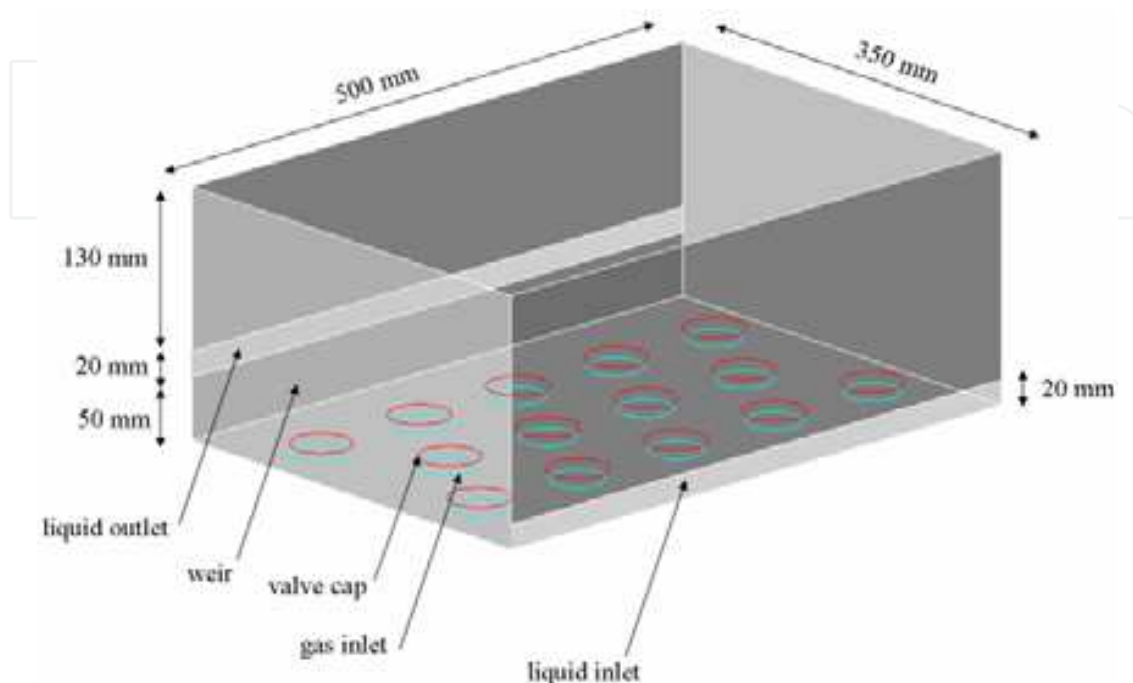


Fig. 1. Schematic of the geometry

The phase-coupled simple (PC-SIMPLE) algorithm, which extends the SIMPLE algorithm to multiphase flows, was applied to determine the pressure-velocity coupling in the simulation. The velocities were solved coupled by phases, but in a segregated fashion. The block algebraic multigrid scheme used by the coupled solver was used to solve a vector equation formed by the velocity components of all phases simultaneously. Then, a pressure correction equation was built based on total volume continuity rather than mass continuity. The pressure and velocities were then corrected to satisfy the continuity constraint. The volume fractions were obtained from the phase continuity equations. To satisfy these conditions, the sum of all volume fractions should be equal to one.

For the continuous phase (liquid phase), the turbulent contribution to the stress tensor was evaluated by the $k-\epsilon$ model described by Sokolichin and Eigenberger (1999) using the following standard single-phase parameters: $C_\mu = 0.09$, $C_{1\epsilon} = 1.44$, $C_{2\epsilon} = 1.92$, $\sigma_K = 1$ and $\sigma_\epsilon = 1.3$.

The discretization scheme for each governing equation involved the following procedure: PC-SIMPLE for the pressure-velocity coupling and "first order upwind" for the momentum, volume fraction, turbulence kinetic energy and turbulence dissipation rate. The under-relaxation factors that determine how much control each of the equations has in the final solution were set to 0.5 for the pressure and volume fraction, 0.8 for the turbulence kinetic energy, turbulence dissipation rate, and for all species.

Using mentioned values for the under-relaxation factors, a reasonable rate of convergence was achieved. The convergence was considered to be achieved when the conservation equations of mass and momentum were satisfied, which was considered to have occurred

when the normalized residuals became smaller than 10^{-3} . The normalization factors used for the mass and momentum were the maximum residual values after the first few iterations.

3.2 Confirmation of grid independency

The results are grid independent. To select the optimized number of grids, a grid independence check was performed. In this test water and air were used as liquid and gas phase, respectively. The flow boundary conditions applied to each phase set the inlet gas velocity to 0.64 ms^{-1} , and the inlet liquid velocity to 0.195 ms^{-1} . Four mesh sizes were examined and results have been represented in table 1. The data were recorded at 15 s, which was the point at which the system stabilized for all cases. Outlet mass flux of air was considered to compare grids. As the difference between numerical results in grid 3 and 4 is less than 0.3%, grid 3 was chosen for the simulation. Figure 2 shows the grid.

Grid	Number of elements	Outlet mass flux of air (g/ s)
1	411×10^3	5.24
2	554×10^3	7.08
3	575×10^3	7.4
4	806×10^3	7.42

Table 1. Results of grid independency

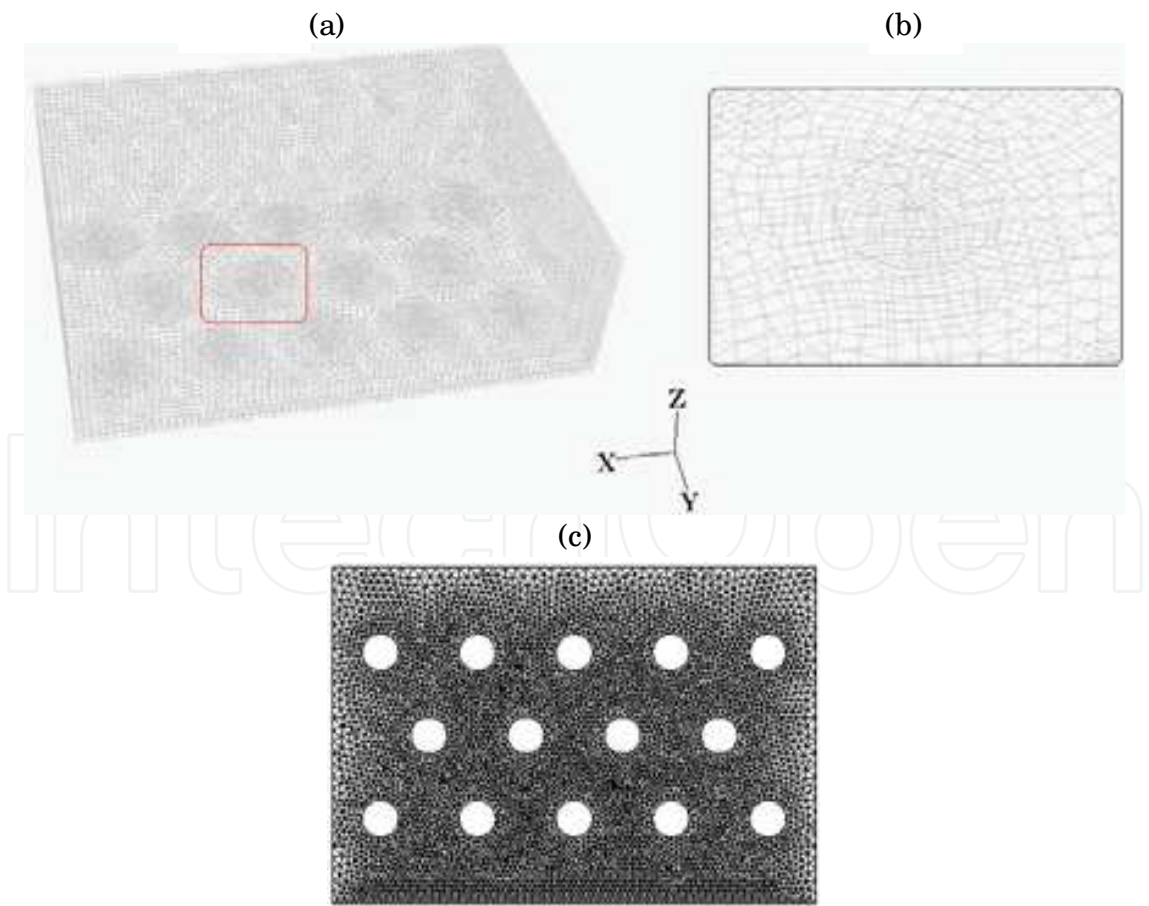


Fig. 2. (a) The grid used in simulations; (b) To obtain better visualization the highlighted part in Fig. 2(a) is magnified; (c) Grid of the tray.

4. Results and discussion

Here hydrodynamics and mass transfer of a distillation column with valve tray is studied. Two-phase, newtonian fluids in Eulerian framework were considered

4.1 Hydrodynamics behaviour of a valve tray

Firstly water and air were used as liquid and gas phase. During the simulation, the clear liquid height, the height of liquid that would exist on the tray in the absence of gas flow, was monitored, and results have been presented in figure 3. As this figure shows, after a sufficiently long time quasi-steady state condition has established. The clear liquid height has been calculated as the tray spacing multiplied by the volume average of the liquid-volume fraction.

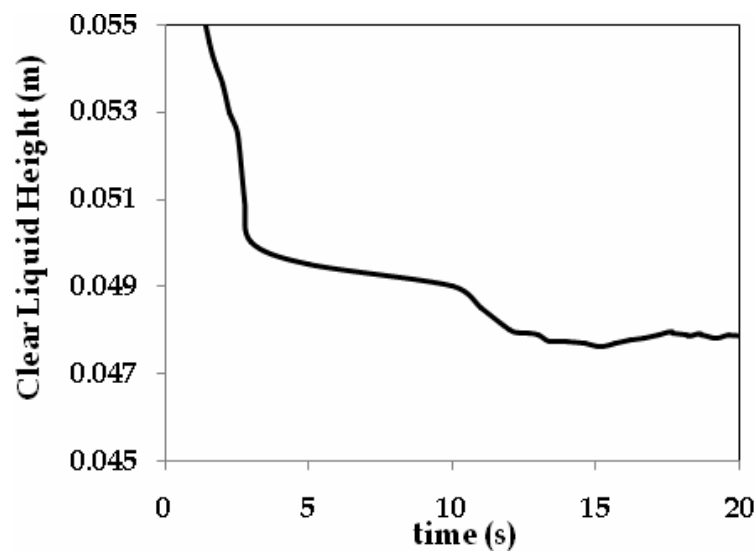


Fig. 3. Clear liquid height versus time.

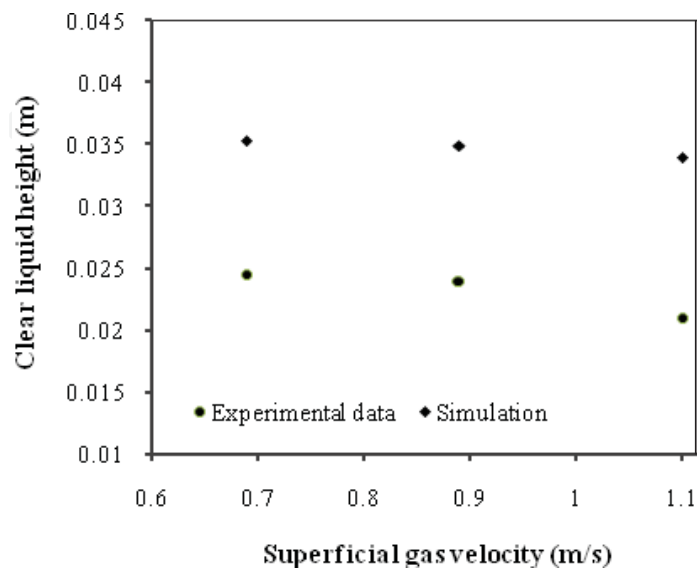


Fig. 4. Clear liquid height as a fuction of superficial gas velocity

In order to valid simulations, results (clear liquid height) were compared with semi-empirical correlations (Li et al., 2009). As figure 3 illustrates, around 15 s steady-state condition is achieved and the clear liquid height is about 0.0478 m. Simulation results are in good agreement with those predicted by semi-empirical correlations and the error is about 2%.

To investigate the effect of gas velocity on clear liquid height, three different velocities (0.69, 0.89 and 1.1 m/s) were applied. The liquid load per weir length was set to $0.0032 \text{ m}^3\text{s}^{-1}\text{m}^{-1}$, and clear liquid height was calculated for the air-water system. Results have been shown in figure 4 and they have been compared with experimental data (Li et al., 2009). As this figure represents, trend of simulations and experimental data are similar.

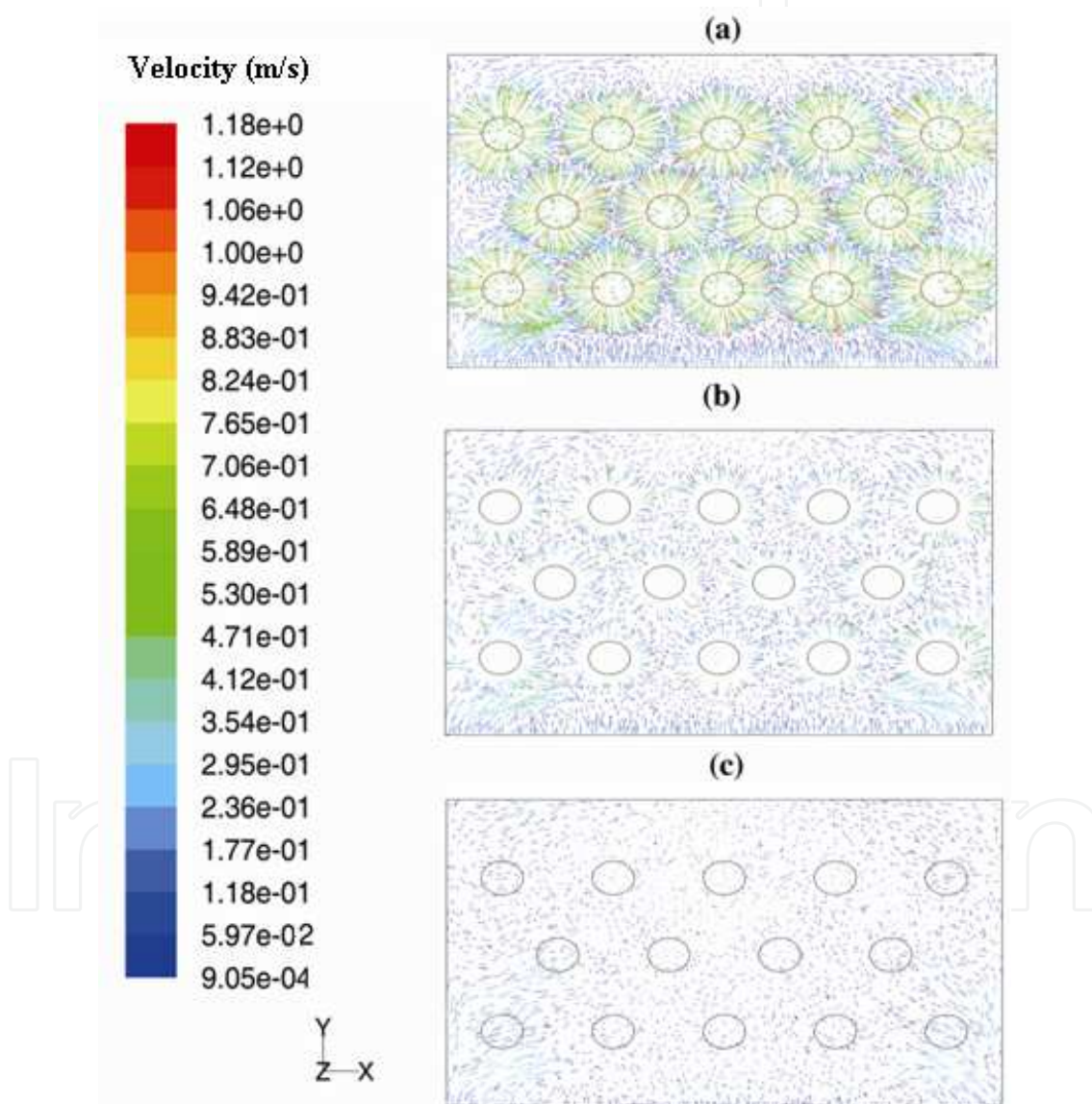


Fig. 5. Top view of liquid velocity vectors after 6 s at (a) $z=0.003\text{m}$, (b) $z=0.009\text{m}$ and (c) $z=0.015\text{m}$.

Simulations continued and two phase containing cyclohexane (C_6H_{12}) and n-heptane (C_7H_{16}) were assumed. Numerical approach has been conducted to reach the stable conditions.

Because flow pattern plays an important role in the tray efficiency; numerical results were analysed and Liquid velocity vectors after 6 s have been represented in figure 5. As this figure illustrates, the circulation of liquid near the tray wall have been observed, confirmed experimentally by Yu & Huang (1980) and also Solari & Bell (1986). In fact, as soon as the liquid enters the tray, the flow passage suddenly expands. This leads to separation of the boundary layer. In turbulent flow, the fluids mix with each other, and the slower flow can easily be removed from the boundary layer and replaced by the faster one. The liquid velocity in lower layers is greater than that in higher layers, thus the turbulent energy of the former is larger, and this leads to the separation point of lower liquid layers moving backward toward the wall. Finally circulation produces in the region near the tray wall.

Gas velocity vectors have been shown in figure 6. As this figure represents, the best mixing of phases happens around caps. Such circulations around valves also have been reported elsewhere (Lianghua et al., 2008). Existence of eddies enhances mixing and has an important effect on mass transfer in a distillation column.

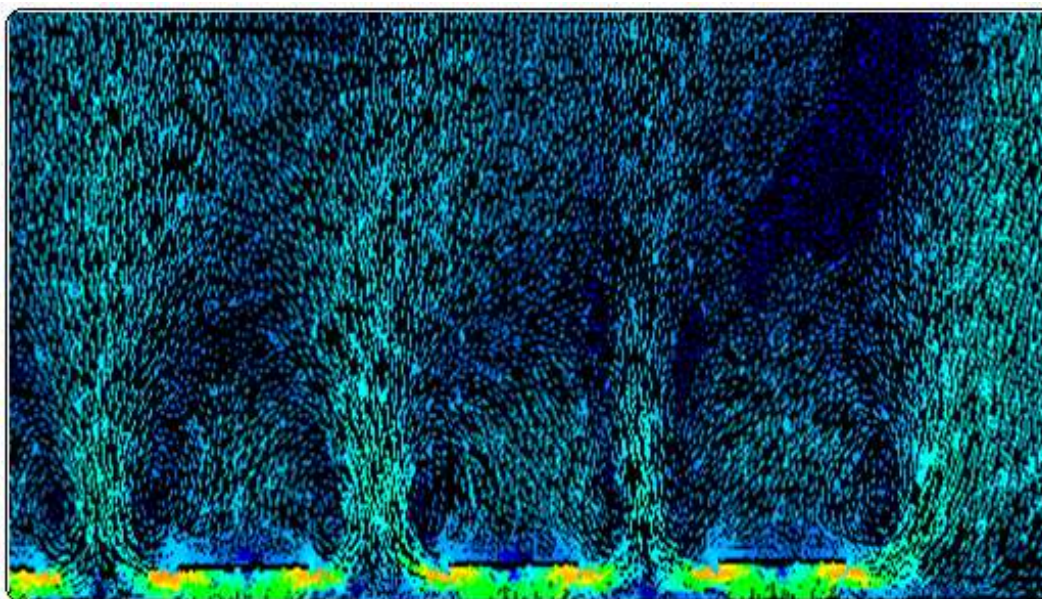


Fig. 6. Gas velocity vectors around caps after 6 s.

4.2 Mass transfer on a valve tray

It is assumed that cyclohexane transfers from liquid to the gas phase, and initial mass fraction of C_7H_{16} in both phases is about 0.15. Concentration is simulated by simultaneously solving the CFD model and mass-transfer equation. Mass fraction of C_7H_{16} in liquid phase versus time has been presented in figure 7. As this figure shows, with passing time mass fraction of n-heptane in liquid increases. In other words, the concentration of the light component (C_6H_{12}) in the gas phase increases along time (figure 8) and the C_7H_{16} concentration in this phase decreases. In addition, C_6H_{12} concentration in gas phase at higher layers increases. Figure 9 shows mass fraction of the light component at three different z and after 6 s. As contours (figure 8 and 9) illustrate, concentrations are not constant over the entire tray and they change point by point. This concept also has been found by Bjorn et al. (2002).

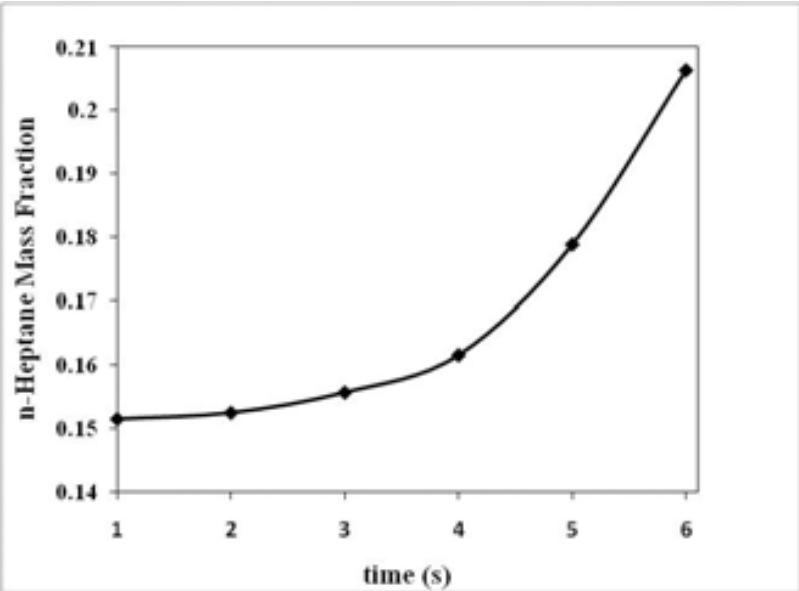


Fig. 7. Changes of n-heptane mass fraction in liquid phase with time.

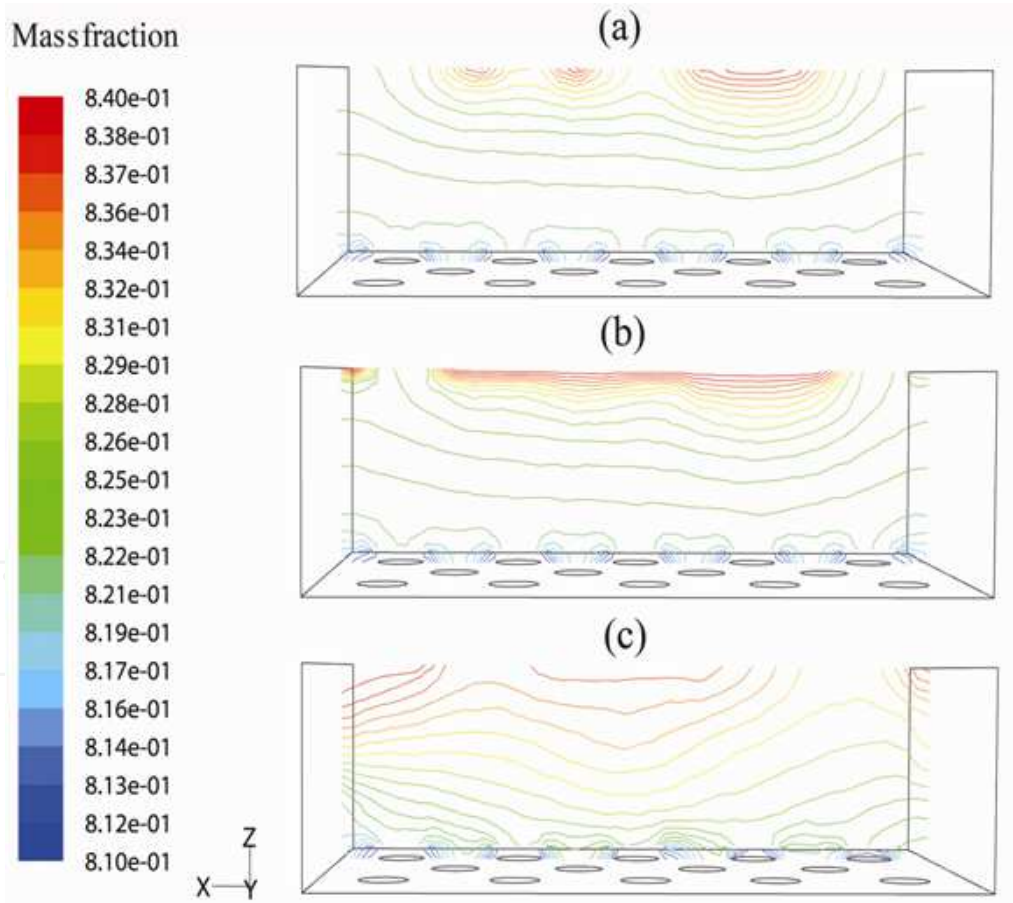


Fig. 8. Mass fraction contours of C_6H_{12} in the gas phase on an x - z plane after (a) 0.25 s, (b) 0.4 s, and (c) 0.6 s.

As mentioned in figure 5, fluid circulation happens near the tray wall. Therefore, the liquid residence time distribution in the same zone is longer than that in other zones. With the

increase of the liquid residence time distribution, mass transfer between gas and liquid is more complete than that in other zones. As the liquid layer moves up, the average concentration of C_6H_{12} in gas phase increases (figure 9) or C_6H_{12} concentration in liquid phase decreases.

A simulation test with high initial velocities of phases were done, and it was found that hydrodynamics have a significant effect on mass transfer. Results of the simulation have been presented in figure 10. Again liquid circulation were observed near the tray wall, and the maximum velocity can be seen around $z=0.009m$ (figure 10 (b)). At this z , C_6H_{12} concentration is in the maximum value and after that the mass fraction becomes constant (figure 10 (c)).

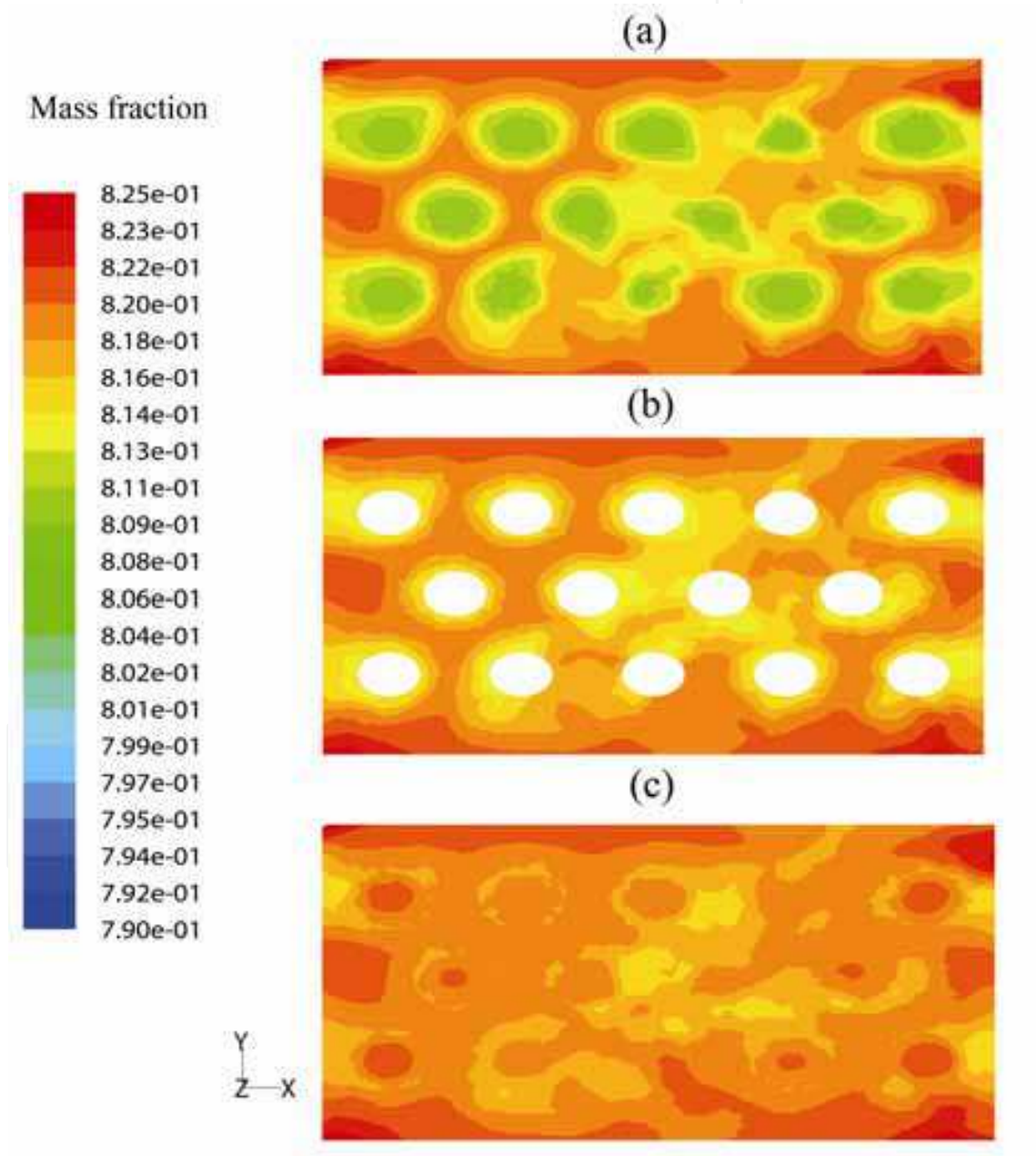


Fig. 9. Mass fraction contours of C_6H_{12} in the gas phase after 6 s at (a) $z=0.003m$; (b) $z=0.009m$ and (c) $z=0.015m$.

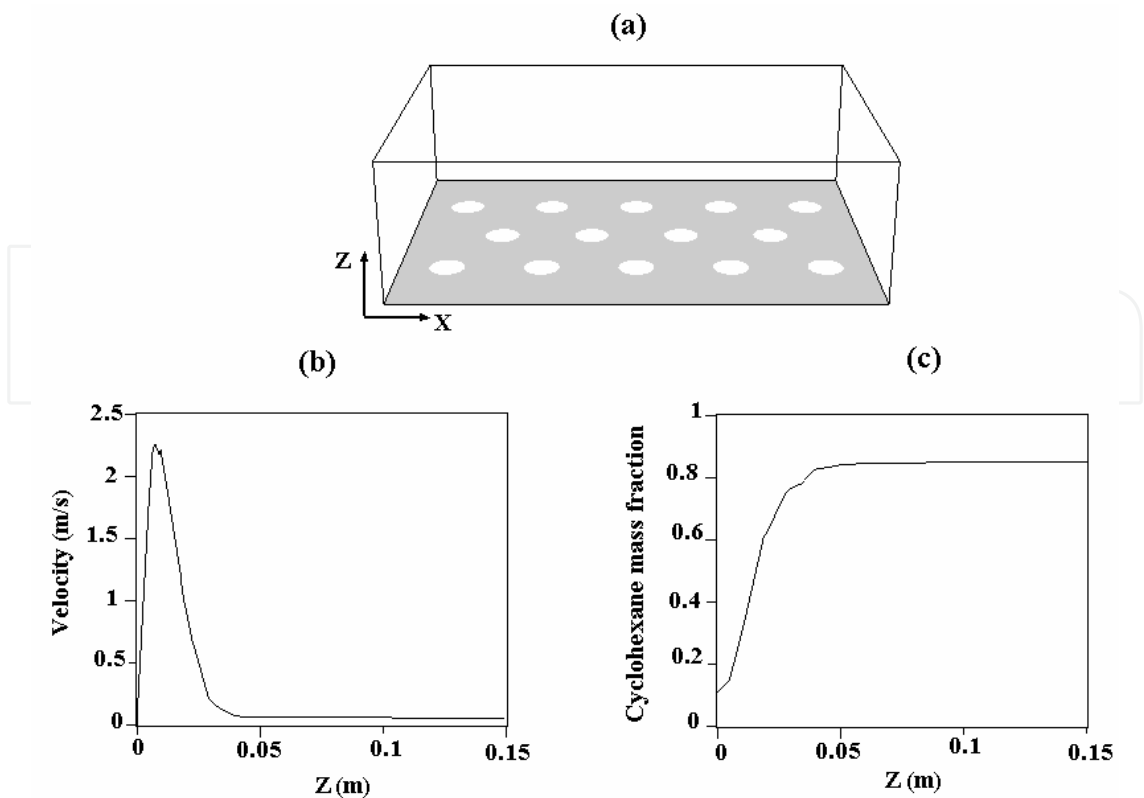


Fig. 10. Results at high initial velocities of gas and liquid after 6s. (a) The geometry; (b) Liquid velocity versus z and (c) Changes of C_6H_{12} mass fraction with z .

Figure 11 represents snapshots of gas hold-up at $z=0$. Fluid hold-up was calculated as the phase volume fraction. Near the tray, gas is dispersed by the continued liquid, and liquid hold-up decreases as height increases.

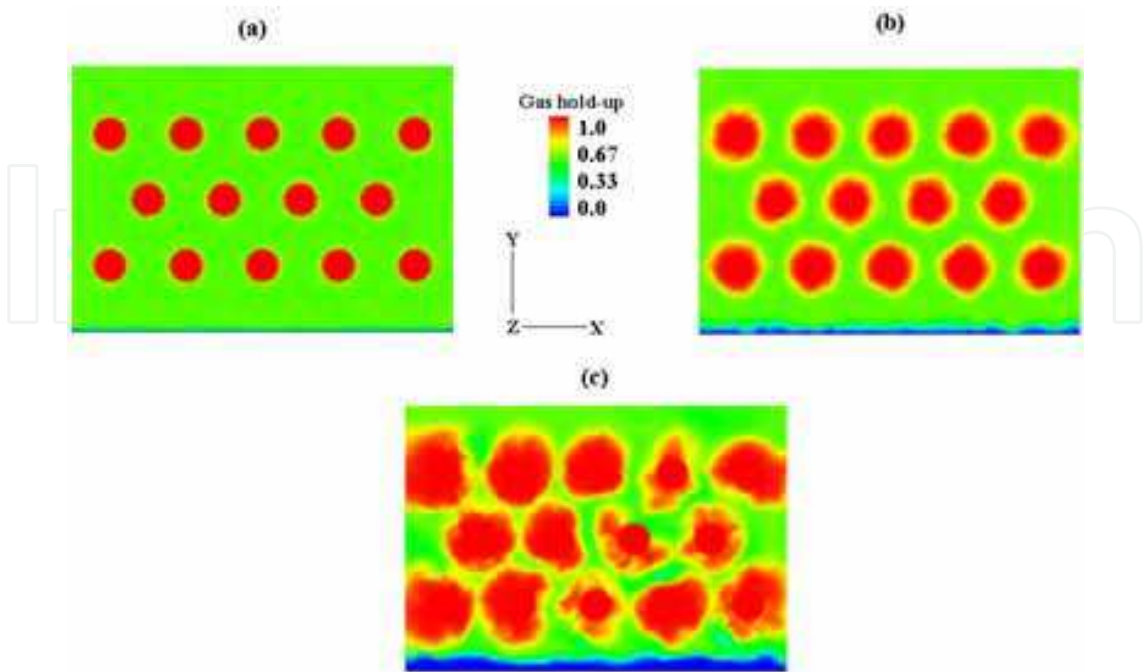


Fig. 11. Gas hold-up at $z=0$ at (a) 1s, (b) 3s, and (c) 6s.

5. Conclusion

A three dimensional two phase flow and mass transfer model was developed for simulation of hydrodynamics behaviour and concentration distribution in a valve tray of a distillation column. CFD techniques have been used and governing equations simultaneously were solved by FLUENT software. Eulerian method was applied in order to predict the behaviour of two phase flow. Clear liquid height for the system of air-water was calculated and results were compared with experimental data.

System of cyclohexane-n-heptane also were considered and its mass transfer were investigated. Eddies near the caps have been observed, and it is found that such circulations enhances mixing and has an important effect on mass transfer in a distillation column. Results show that the concentration of the light component (C_6H_{12}) in the vapour phase increases along time and the C_7H_{16} concentration in the vapour phase decreases. In addition, concentrations are not constant over the entire tray and they change point by point. This research showed that CFD is a powerful technique in design and analysis of mass transfer in distillation columns and the presented model can be used for further study about mass transfer of valve trays.

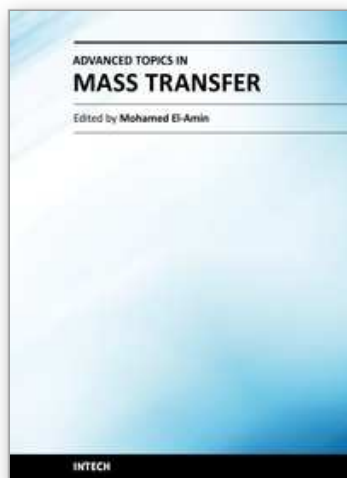
6. Acknowledgements

The authors thank the National Iranian Oil Refining & Distribution Company (NIORDC) because of financial support of this research (contract No. 88-1096). Special thanks to Eng. Mohammad Reza Mirian for his kind cooperation in this work.

7. References

- Alizadehdakhel, A.; Rahimi, M. & Abdulaziz Alsairafi, A. (2010). CFD and experimental studies on the effect of valve weight on performance of a valve tray column. *Comp. Chem. Eng.*, 34, 1–8.
- Bjorn, I.N.; Gren, U. & Svensson, F. (2002). Simulation and experimental study of intermediate heat exchange in a sieve tray distillation column. *Comp. Chem. Eng.*, 26, 499-505.
- Buwa, V.V. & Ranade, V.V. (2002). Dynamics of gas-liquid flow in a rectangular bubble column: Experiments and single/ multi-group CFD simulations. *Chem. Eng. Sci.*, 57, 22, 4715-4736.
- C.H. Fischer & G.L. Quarini, 1998. Three-dimensional heterogeneous modelling of distillation tray hydraulics. Paper presented at the AIChE Annual Meeting, Miami Beach, FL, 15-19.
- Deen, N.G.; Solberg, T. & Hjertager, B.H. (2001). Large eddy simulation of the gas-liquid flow in a square cross-sectioned bubble column. *Chem. Eng. Sci.*, 56, 6341-6349.
- Delnoij, E.; Kuipers, J.A.M. & van Swaaij, W.P.M. (1999). A three-dimensional CFD model for gas-liquid bubble columns. *Chem. Eng. Sci.*, 54, 13/ 14, 2217-2226.
- Fluent 6.2 Users Guide (2005). Fluent Inc., Lebanon.
- Hirschberg, S.; Wijn, E.F. & Wehrli, M. (2005). Simulating the two phase flow on column trays. *Chem. Eng. Res. Des.*, 83, A12, 1410–1424.
- Krishna, R.; Van Baten, J.M.; Ellenberger, J.; Higler, A.P. & Taylor, R. (1999). CFD simulations of sieve tray hydrodynamics. *Chem. Eng. Res. Des.*, 77, 639–646.

- Li, X.G.; Liuc, D.X.; Xua, Sh.M. & Li, H. (2009). CFD simulation of hydrodynamics of valve tray. *Chem. Engin. Proc.*, 48, 145–151.
- Lianghua, W.; Juejian, C. & Kejian, Y. (2008). Numerical simulation and analysis of gas flow field in serrated valve column. *Chin. J. of Chem. Eng.*, 16, 4, 541-546.
- Ling Wang, X.; Jiang Liu, C.; Gang Yuan, X. & Yu, K.T. (2004). Computational fluid dynamics simulation of three-dimensional liquid flow and mass transfer on distillation column trays. *Ind. Eng. Chem. Res.*, 43, 2556-2567.
- Liu, C.J.; Yuan, X.G.; Yu, K.T. & Zhu, X.J (2000). A fluid-dynamics model for flow pattern on a distillation tray. *Chem. Eng. Sci.*, 55, 12, 2287-2294.
- McFarlane, R.C.; Muller, T.D. & Miller, F.G. (1967). Unsteady-state distribution of fluid composition in two-phase oil reservoirs undergoing gas injection. *Soc. Petrol. Eng. J.*, 7, 1, 61-74.
- Mehta, B.; Chuang, K.T. & Nandakumar, K. (1998). Model for liquid phase flow on sieve trays. *Chem. Engin. Res. and Des.*, 76, 843-848.
- Rahbar, R.; Rahimi, M.R.; Shahraki, F. & Zivdar, M. (2006). Efficiencies of sieve tray distillation columns by CFD simulation. *Chem. Eng. Technol.*, 29, 3, 326-335.
- Sanyal, J.; Marchisio, D.L.; Fox, R.O. & Dhanasekharan, K. (2005). On the comparison between population balance models for CFD simulation of bubble columns. *Ind. Eng. Chem. Res.*, 44, 14, 5063-5072.
- Solari, R.B.; Bell, R.L. (1986). Fluid flow patterns and velocity distribution on commercial-scale sieve trays. *AIChE J.*, 32, 4, 640-649.
- Sokolichin, A.; Eigenberger, G.; (1999). Applicability of the standard turbulence model to the dynamic simulation of bubble columns. Part I. Detailed numerical simulations, *Chem. Eng. Sci.*, 54, 2273–2284.
- Sun, Z.M.; Yu, K.T.; Yuan, X.G.; Liu, C.J & Sun, Z.M. (2007). A modified model of computational mass transfer for distillation column. *Chem. Eng. Sci.*, 62, 1839 – 1850.
- Van Baten, J.M. & Krishna, R. (2000). Modelling sieve tray hydraulics using computational fluid dynamics. *Chem. Eng. J.*, 77, 3, 143-151.
- We, C.; Farouqali, S.M. & Stahl, C.D. (1969). Experimental and numerical simulation of two-phase flow with interface mass transfer in one and two dimensions. *Soc. Petrol. Eng. J.*, 9, 3, 323-337.
- Wijn, E.F. (1996). The effect of downcomer layout pattern on tray efficiency. *Chem. Eng. J.*, 63, 167-180.
- Xigang, Y. & Guocong, Y. (2008). Computational mass transfer method for chemical process simulation. *Chin. J. of Chem. Eng.*, 16, 4, 497-502.
- YOU, X.Y. (2004). Numerical simulation of mass transfer performance of sieve distillation trays. *Chem. Biochem. Eng. Q.*, 18, 3, 223–233.
- Yu, K.T.; Huang, J (1980). Simulation of large tray and tray efficiency. *Paper presented at the AIChE Spring National Meeting, Philadelphia.*
- Yu, K.T.; Yuan, X.G.; You, X.Y. & Liu, C.J (1999). Computational fluid-dynamics and experimental verification of two-phase two dimensional flow on a sieve column tray. *Chem. Eng. Res. Des.*, 77A, 554-558.
- Zhang, M.Q. & Yu, K.T. (1994). Simulation of two-dimensional liquid flow on a distillation tray. *Chin. J. Chem. Eng.*, 2, 2, 63-71.



Advanced Topics in Mass Transfer

Edited by Prof. Mohamed El-Amin

ISBN 978-953-307-333-0

Hard cover, 626 pages

Publisher InTech

Published online 21, February, 2011

Published in print edition February, 2011

This book introduces a number of selected advanced topics in mass transfer phenomenon and covers its theoretical, numerical, modeling and experimental aspects. The 26 chapters of this book are divided into five parts. The first is devoted to the study of some problems of mass transfer in microchannels, turbulence, waves and plasma, while chapters regarding mass transfer with hydro-, magnetohydro- and electro- dynamics are collected in the second part. The third part deals with mass transfer in food, such as rice, cheese, fruits and vegetables, and the fourth focuses on mass transfer in some large-scale applications such as geomorphologic studies. The last part introduces several issues of combined heat and mass transfer phenomena. The book can be considered as a rich reference for researchers and engineers working in the field of mass transfer and its related topics.

How to reference

In order to correctly reference this scholarly work, feel free to copy and paste the following:

A. Jafari, S.M. Mousavi, H. Motesaffi, H. Roohian and H. Hamed Sangari (2011). Simulation of Hydrodynamics and Mass Transfer in a Valve Tray Distillation Column Using Computational Fluid Dynamics Approach, Advanced Topics in Mass Transfer, Prof. Mohamed El-Amin (Ed.), ISBN: 978-953-307-333-0, InTech, Available from: <http://www.intechopen.com/books/advanced-topics-in-mass-transfer/simulation-of-hydrodynamics-and-mass-transfer-in-a-valve-tray-distillation-column-using-computational-fluid-dynamics-approach>

INTECH
open science | open minds

InTech Europe

University Campus STeP Ri
Slavka Krautzeka 83/A
51000 Rijeka, Croatia
Phone: +385 (51) 770 447
Fax: +385 (51) 686 166
www.intechopen.com

InTech China

Unit 405, Office Block, Hotel Equatorial Shanghai
No.65, Yan An Road (West), Shanghai, 200040, China
中国上海市延安西路65号上海国际贵都大饭店办公楼405单元
Phone: +86-21-62489820
Fax: +86-21-62489821

© 2011 The Author(s). Licensee IntechOpen. This chapter is distributed under the terms of the [Creative Commons Attribution-NonCommercial-ShareAlike-3.0 License](https://creativecommons.org/licenses/by-nc-sa/3.0/), which permits use, distribution and reproduction for non-commercial purposes, provided the original is properly cited and derivative works building on this content are distributed under the same license.

IntechOpen

IntechOpen